A toolbox for lattice-spin models with polar molecules

A. MICHELI*, G. K. BRENNEN AND P. ZOLLER

Institute for Theoretical Physics, University of Innsbruck, and Institute for Quantum Optics and Quantum Information of the Austrian Academy of Science, 6020 Innsbruck, Austria

***e-mail: andrea.micheli@uibk.ac.at**

Published online: 30 April 2006; doi:10.1038/nphys287

There is growing interest in states of matter with topological order. These are characterized by highly stable ground states robust to perturbations that preserve the topology, and which support excitations with so-called anyonic statistics. Topologically ordered states can arise in two-dimensional lattice-spin models, which were proposed as the basis for a new class of quantum computation. Here, we show that the relevant hamiltonians for such spin lattice models can be systematically engineered with polar molecules stored in optical lattices, where the spin is represented by a single-valence electron of a heteronuclear molecule. The combination of microwave excitation with dipole–dipole interactions and spin–rotation couplings enables building a complete toolbox for effective two-spin interactions with designable range, spatial anisotropy and coupling strengths significantly larger than relevant decoherence rates. Finally, we illustrate two models: one with an energy gap providing for error-resilient qubit encoding, and another leading to topologically protected quantum memory.

Lattice-spin models are ubiquitous in condensed-matter physics, where they are used as simplified models to describe the characteristic behaviour of more-complicated interacting physical systems. Recently there have been exciting theoretical discoveries of models with quasi-local spin interactions with emergent topological order[1,2]. In contrast to Landau theory where various phases of matter are described by broken symmetries, topological ordered states are distinguished by a homology class and have the property of being robust to arbitrary perturbations of the underlying hamiltonian. These states do not exhibit long-range order in pairwise operators, but rather they have long-range order in highly non-local strings of operators. A real-world example is the fractional quantum Hall effect, which gives rise to states with the same symmetry but distinguishable by quantum numbers associated with the topology of the surface they live on[3].

It is of significant interest to 'design' materials with these properties, both to observe and to study exotic phases, and in the light of possible applications. Cold atomic and molecular gases in optical lattices are prime candidates for this endeavour in view of the complete controllability of these systems in the laboratory. The idea of realizing bosonic and fermionic Hubbard models, and thus also lattice-spin models, with cold atoms in optical lattices has sparked a remarkable series of experiments, and has triggered numerous theoretical studies to develop cold atoms as a quantum simulator for strongly correlated condensed-matter systems[4–6]. However, coaxing a physical system to mimic the required interactions for relevant lattice-spin models, which must be both anisotropic in space and in the spin degrees of freedom and a given range, is highly non-trivial. Here, we show that cold gases of polar molecules, as currently developed in the laboratory[7], allow us to construct, in a natural way, a complete toolbox for any permutation-symmetric two-spin-1/2 (qubit) interaction. The attraction of this idea also rests on the fact that dipolar interactions have coupling strengths significantly larger than those of the atomic Hubbard models, and than relevant decoherence rates.

Our basic building block is a system of two polar molecules strongly trapped at given sites of an optical lattice, where the spin-1/2 (or qubit) is represented by a single electron outside a closed shell of a heteronuclear molecule in its rotational ground state. Heteronuclear molecules have large permanent electric dipole moments. This implies that the rotational motion of molecules

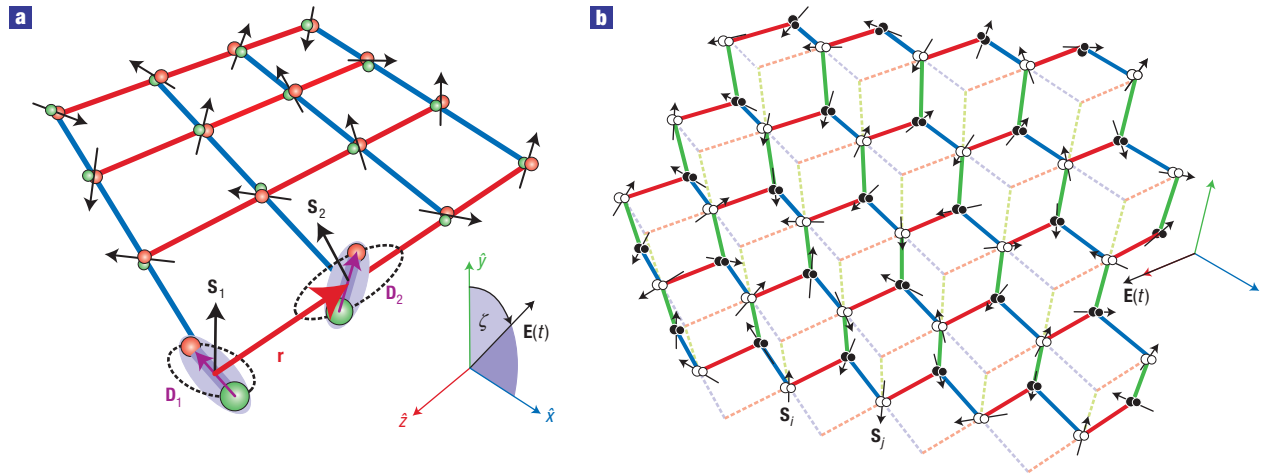

Figure 1 Example anisotropic spin models that can be simulated with polar molecules trapped in optical lattices. a, Square lattice in 2D with nearest-neighbour orientation-dependent Ising interactions along $\hat{x}$ and $\hat{z}$. Effective interactions between the spins $\mathbf{S}_1$ and $\mathbf{S}_2$ of the molecules in their rovibrational ground states are generated with a microwave field $\mathbf{E}(t)$ inducing dipole–dipole interactions between the molecules with dipole moments $\mathbf{D}_1$ and $\mathbf{D}_2$, respectively. **b**, Two staggered triangular lattices with nearest neighbours oriented along orthogonal triads. The interactions depend on the orientation of the links with respect to the electric field. (Dashed lines are included for perspective.)

is coupled strongly through the dipole–dipole interactions, whose signatures are the long-range $1/r^3$ character and an angular dependence, where the polar molecules attract or repel each other depending on the relative orientation of their dipole moments. In addition, microwave excitation of rotational energy levels allows us to effectively tailor the spatial dependence of dipole–dipole interactions. Finally, accounting for the spin–rotation splitting of molecular rotational levels, we can make these dipole–dipole interactions spin-dependent. General lattice-spin models are readily built from these binary interactions.

ANISOTROPIC SPIN MODELS WITH NOISE-RESILIENT GROUND STATES

Two highly anisotropic models with spin-1/2 particles, which we will show how to simulate, are illustrated in Fig. 1a and b respectively. The first model takes place on a square 2D lattice with nearest-neighbour interactions

$$H_{\mathrm{spin}}^{(\mathrm{I})} = \sum_{i=1}^{\ell-1}\sum_{j=1}^{\ell-1} J(\sigma_{i,j}^{z}\sigma_{i,j+1}^{z} + \cos\zeta\,\sigma_{i,j}^{x}\sigma_{i+1,j}^{x}).$$

Introduced by Duoçot *et al.*[8] in the context of Josephson junction arrays, this model (for $\zeta \neq \pm\pi/2$) admits a twofold degenerate ground subspace that is immune to local noise up to ℓth order, and hence is a good candidate for storing a protected qubit.

The second model occurs on a bipartite lattice constructed with two 2D triangular lattices, one shifted and stacked on top of the other. The interactions are indicated by nearest-neighbour links along the $\hat{x}$, $\hat{y}$ and $\hat{z}$ directions in real space:

$$H_{\mathrm{spin}}^{(\mathrm{II})} = J_{\perp}\sum_{x\text{-links}}\sigma_j^x\sigma_k^x + J_{\perp}\sum_{y\text{-links}}\sigma_j^y\sigma_k^y + J_z\sum_{z\text{-links}}\sigma_j^z\sigma_k^z.$$

This model has the same spin dependence and nearest-neighbour graph as the model on a honeycomb lattice introduced by Kitaev[9]. He has shown that by adjusting the ratio of interaction strengths $|J_{\perp}|/|J_z|$ the system can be tuned from a gapped phase carrying abelian anyonic excitations to a gapless phase that, in the presence of a magnetic field, becomes gapped with non-abelian excitations. In the regime $|J_{\perp}|/|J_z| \ll 1$ the hamiltonian can be mapped to a model with four-body operators on a square lattice with ground states that encode topologically protected quantum memory[10]. One proposal[11] describes how to use trapped atoms in spin-dependent optical lattices to simulate the spin model $H_{\mathrm{spin}}^{(\mathrm{II})}$. There the induced spin couplings are obtained through spin-dependent collisions in second-order tunnelling processes. Larger coupling strengths are desirable. In both spin models (I and II) above, the signs of the interactions are irrelevant, although we will be able to tune the signs if needed.

SPECTROSCOPY OF POLAR MOLECULES IN OPTICAL LATTICES

Our system comprises heteronuclear molecules with ${}^2\Sigma_{1/2}$ ground electronic states, corresponding, for example, to alkaline-earth monohalides with a single electron outside a closed shell. We adopt a model molecule where the rotational excitations are described by the hamiltonian $H_{\mathrm{m}} = B\mathbf{N}^2 + \gamma\mathbf{N}\cdot\mathbf{S}$, with $\mathbf{N}$ being the dimensionless orbital angular momentum of the nuclei, and $\mathbf{S}$ being the dimensionless electronic spin (assumed to be $S = 1/2$ in the following). Here B denotes the rotational constant and γ is the spin–rotation coupling constant, where a typical B is a few tens of GHz, and γ is in the hundred MHz regime. The coupled basis of a single molecule i corresponding to the eigenbasis of H_{m}^i is $\{|N_i, S_i, J_i; M_{J_i}\rangle\}$, where $\mathbf{J}_i = \mathbf{N}_i + \mathbf{S}_i$ with eigenvalues $E(N=0, S=1/2, J=1/2) = 0, E(1, 1/2, 1/2) = 2B - \gamma$, and $E(1, 1/2, 3/2) = 2B + \gamma/2$. Although we ignore hyperfine interactions in the present work, our discussion below is readily extended to include hyperfine effects, which offer extensions to spin systems $S > 1/2$.

The hamiltonian describing the internal and external dynamics of a pair of molecules trapped in wells of an optical lattice is denoted by $H = H_{\mathrm{in}} + H_{\mathrm{ex}}$. The interaction describing the internal degrees of freedom is $H_{\mathrm{in}} = H_{\mathrm{dd}} + \sum_{i=1}^{2} H_{\mathrm{m}}^i$. Here H_{dd} is the dipole–dipole interaction given below in equation (1).

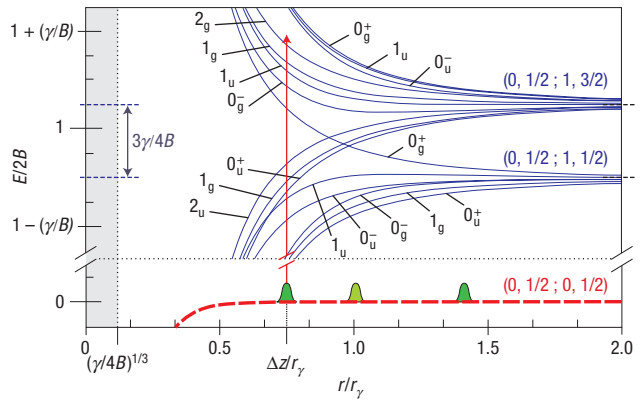

Figure 2 Movre–Pichler potentials for a pair of molecules as a function of their separation *r*. The potentials $E(g_i(r))$ for the four ground states (dashed lines) and the potentials $E(\lambda(r))$ for the first 24 excited states (solid lines). The symmetries $|Y|^{\pm}_{\sigma}$ of the corresponding excited manifolds are indicated, as are the asymptotic manifolds (N_i, J_i; N_j, J_j). The relative coordinate probability densities on a square lattice are depicted in green on the ground-state potentials. The red arrow indicates the coupling of the microwave field.

The hamiltonian describing the external, or motional, degrees of freedom is $H_{\rm ex}=\sum_{i=1}^{2}\mathbf{P}_i^2/(2m)+V_i(\mathbf{x}_i-\bar{\mathbf{x}}_i)$, where $\mathbf{P}_i$ is the momentum of molecule i with mass m, and the potential generated by the optical lattice $V_i(\mathbf{x}-\bar{\mathbf{x}}_i)$ describes an external confinement of molecule i about a local minimum $\bar{\mathbf{x}}_i$ with 1D r.m.s. width z_0. We assume isotropic traps that are approximately harmonic near the trap minimum with a vibrational spacing $\hbar\omega_{\rm osc}$. Furthermore, we assume that the molecules can be prepared in the motional ground state of each local potential using dissipative electromagnetic pumping[12], perhaps beginning with a two-species Mott insulator[13]. It is convenient to define the quantization axis $\hat{z}$ along the axis connecting the two molecules, $\bar{\mathbf{x}}_2-\bar{\mathbf{x}}_1=\Delta z\hat{z}$ with Δz corresponding to a multiple of the lattice spacing.

The near-field dipole–dipole interaction between two molecules separated by $\mathbf{r}=\mathbf{x}_1-\mathbf{x}_2$ is

$$H_{\rm dd}=\frac{d^2}{r^3}\left(\sum_{q=-1}^{q=1}(-1)^q D_{1q}^{\dagger}D_{2-q}-3D_{10}^{\dagger}D_{20}+\text{h.c.}\right). \qquad (1)$$

The dipole operator coupling the ground and first rotational states of molecule i is $\mathbf{D}_i^{\dagger}=\sum_{q=-1}^{1}|N=1,q\rangle_{ii}\langle N=0,0|\hat{e}_q^{*}$, with the spherical basis vectors $\{\hat{e}_0=\hat{z},\hat{e}_{\pm1}=\mp(\hat{x}\pm i\hat{y})/\sqrt{2}\}$, and d is the dimensionful dipole moment.

Although the present situation of dipole–dipole coupling of rotationally excited polar molecules is reminiscent of the dipole–dipole interaction between electronically excited atom pairs[14], there are important differences. First, unlike the atomic case where electronically excited states are typically anti-trapped by an optical lattice, here both ground and excited rotational states are trapped by an essentially identical potential up to tensor shifts[15,16], which can be compensated by applying a static electric field. Hence, motional decoherence due to spin-dependent dipole–dipole forces is strongly suppressed by the large vibrational energy $\hbar\omega_{\rm osc}$. Second, spontaneous emission rates are drastically reduced. The decay rate at room temperature from excited rotational states is $\sim10^{-3}$ Hz (ref. 17) versus a comparable rate of MHz for excited electronic states. There are other, stronger, sources of decoherence, the most important being photon scattering from the optical trapping laser. For reasonable traps the scattering rate can be of the order of 0.2 Hz (ref. 16).

The ground subspace of each molecule is isomorphic to a spin-1/2 particle. Our goal is to obtain an effective spin–spin interaction between two neighbouring molecules. Static spin–spin interactions due to spin–rotation and dipole–dipole couplings do exist but are very small in our model: $H_{\rm vdW}(r)=-(3d^4/2Br^6)\left[1+(\gamma/4B)^2\left(1+4\mathbf{S}_1\cdot\mathbf{S}_2/3-2S_1^zS_2^z\right)\right]$. The first term is the familiar van der Waals $1/r^6$ interaction, whereas the spin-dependent piece is strongly suppressed as $\gamma/4B\approx10^{-3}\ll1$. Therefore, we propose dynamical mixing with dipole–dipole coupled excited states using a microwave field.

The molecules are assumed trapped with a separation $\Delta z\sim r_\gamma\equiv(2d^2/\gamma)^{1/3}$, where the dipole–dipole interaction is $d^2/r_\gamma^3=\gamma/2$. In this regime, the rotation of the molecules is strongly coupled to the spin. The ground states are essentially spin-independent, and the excited states are described by Hund's case-(c) states in analogy to the dipole–dipole coupled excited electronic states of two atoms with fine structure. Remarkably, as described in the Methods section, the eigenvalues and eigenstates of $H_{\rm in}$ can be computed analytically yielding the well-known Movre–Pichler potentials[18] plotted in Fig. 2.

Possible candidate polar molecules are, for example, CaF, CaCl and MgCl. The rotational constant, spin–rotation coupling constant and dipole moment are: CaF ($B/h=10.304$ GHz, $\gamma/h=39.66$ MHz, $d\sqrt{3}=3.07$ D), $Ca^{35}Cl$ ($B/h=4.565$ GHz, $\gamma/h=42.21$ MHz, $d\sqrt{3}=4.27$ D) and $^{26}Mg^{35}Cl$ ($B/h=7.005$ GHz, $\gamma/h=63.52$ MHz, $d\sqrt{3}=3.38$ D). With a typical optical lattice spacing of $\Delta z\sim300$ nm, it would be difficult to trap near r_γ. However, we note that it is possible to resolve many excited states even at larger intermolecular spacings. In the Methods section, we describe how the two spin models considered here can be implemented at the cost of smaller effective interaction strengths.

ENGINEERING SPIN–SPIN INTERACTIONS

To induce strong dipole–dipole coupling, we introduce a microwave field $E(\mathbf{x},t)\mathbf{e}_{\rm F}$ with a frequency $\omega_{\rm F}$ tuned near resonance with the $N=0\rightarrow N=1$ transition. Because the rotational states are spaced nonlinearly, this transition is resolvable without coupling to higher rotational states by multiphoton processes. In the rotating-wave approximation, the molecule–field interaction is $H_{\rm mf}=-\sum_{i=1}^{2}(\hbar\Omega\mathbf{D}_i^{\dagger}\cdot\mathbf{e}_{\rm F}e^{i(\mathbf{k}_{\rm F}\cdot\mathbf{x}_i-\omega_{\rm F}t)}/2+\text{h.c.})$, where the Rabi frequency is $|\Omega|=d|E_0|/\hbar$. For molecules spaced by optical wavelengths, all the dipoles are excited in phase.

The effective hamiltonian acting on the ground states is obtained in second-order perturbation theory as

$$H_{\rm eff}(r)=\sum_{i,f}\sum_{\lambda(r)}\frac{\langle g_f|H_{\rm mf}|\lambda(r)\rangle\langle\lambda(r)|H_{\rm mf}|g_i\rangle}{\hbar\omega_{\rm F}-E(\lambda(r))}|g_f\rangle\langle g_i|, \qquad (2)$$

where $\{|g_i\rangle,|g_f\rangle\}$ are ground states with $N_1=N_2=0$ and $\{|\lambda(r)\rangle\}$ are excited eigenstates of $H_{\rm in}$ with $N_1+N_2=1$ and with excitation energies $\{E(\lambda(r))\}$. The reduced interaction in the subspace of the spin degrees of freedom is then obtained by tracing over the motional degrees of freedom. For molecules trapped in the ground motional states of isotropic harmonic wells with r.m.s. width z_0, the wavefunction is separable in centre-of-mass and relative coordinates with the relative-coordinate wavefunction

$$\psi_{\rm rel}(r,\theta)=\frac{1}{\pi^{3/4}(2z_0)^{3/2}}e^{-(r^2+\Delta z^2-2r\Delta z\cos\theta)/8z_0^2},$$

where $\cos\theta=\mathbf{r}\cdot\hat{z}/r$. The effective spin–spin hamiltonian is then $H_{\rm spin}=\langle H_{\rm eff}(r)\rangle_{\rm rel}$.

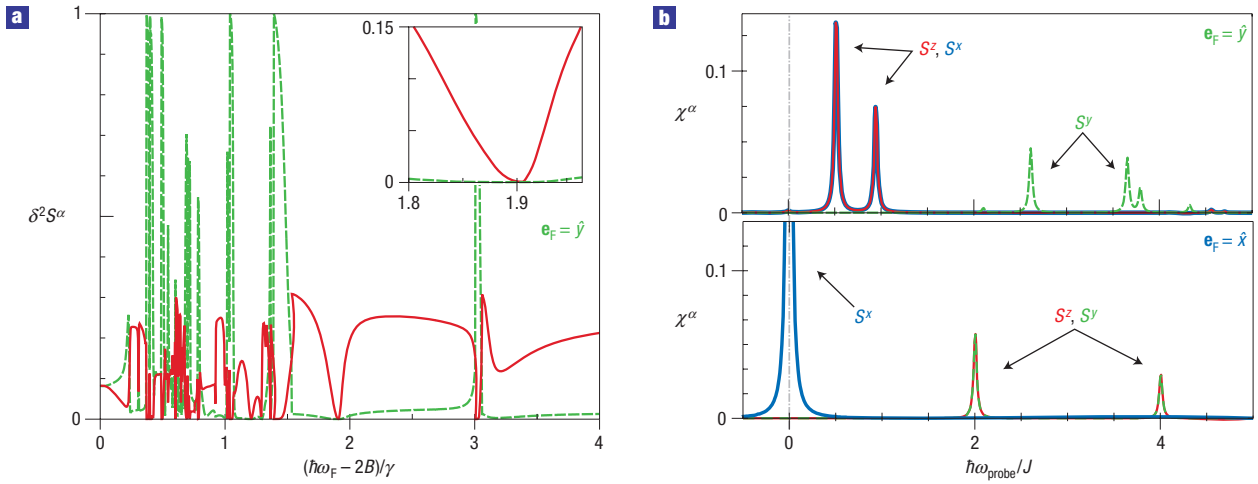

Figure 3 Design and verification of noise-protected ground states arising from a simulation of $H^{(I)}_{spin}$. The system comprises nine molecules trapped in a 3×3 lattice in the $\hat{z}$–$\hat{x}$ plane with lattice spacing $b = r_\gamma/\sqrt{2}$ driven with a field of frequency ω_F and out-of-plane polarization angle ζ. **a**, Noise resilience of the ground states as a function of ω_F, quantified by the r.m.s. magnetizations of the two ground states, $\delta^2 S^z = \delta^2 S^x$ (solid red lines) and $\delta^2 S^y$ (dashed green lines) for $\zeta = 0$. The inset shows the protected region, when tuning near the 2_g resonance $E(2_g) \approx 1.9\gamma$, which realizes $H^{(I)}_{spin}$. **b**, Absorption spectroscopy of ground states $\chi^\alpha(\omega_{probe})$ for two spin textures obtained by tuning ω_F near the 2_g resonance at $\hbar\omega_F - 2B = 1.88\gamma$. For $\zeta = 0$ the spectrum is gapped by $J/2$, which is a signature of a protected qubit (top), whereas for $\zeta = \pi/2$ the excitations are gapless spin waves (bottom).

The hamiltonian in equation (2) is guaranteed to yield some entangling interaction for appropriate choices of field parameters, but it is desirable to have a systematic way to design a spin–spin interaction. Fortunately, the model presented here possesses sufficient structure to achieve this essentially analytically. The effective hamiltonian on molecules 1 and 2 induced by a microwave field is

$$H_{\rm eff}(r) = \frac{\hbar|\Omega|}{8} \sum_{\alpha,\beta=0}^{3} \sigma_1^\alpha A_{\alpha,\beta}(r) \sigma_2^\beta, \qquad (3)$$

where $\{\sigma^\alpha\}_{\alpha=0}^3 \equiv \{\mathbf{1}, \sigma^x, \sigma^y, \sigma^z\}$ and A is a real symmetric tensor. See the Methods section for an explicit form of the matrix coefficients as a function of field polarization and frequency.

Equation (3) describes a generic permutation-symmetric two-qubit hamiltonian. The components $A_{0,s}$ describe a pseudo-magnetic field that acts locally on each spin, and the components $A_{s,t}$ describe two-qubit coupling. The pseudo-magnetic field is zero if the microwave field is linearly polarized, but a real magnetic field could be used to tune local interactions and, given a large enough gradient, could break the permutation invariance of $H_{\rm spin}$.

For a given field polarization, tuning the frequency near an excited state induces a particular spin pattern on the ground states. These patterns change as the frequency is tuned though multiple resonances at a fixed intermolecular separation. In Table 1, it is shown how to simulate the Ising and Heisenberg interactions in this way. Using several fields that are sufficiently separated in frequency, the resulting effective interactions are additive, creating a spin texture on the ground states. The anisotropic spin model $H_{XYZ} = \lambda_x \sigma^x \sigma^x + \lambda_y \sigma^y \sigma^y + \lambda_z \sigma^z \sigma^z$ can be simulated using three fields: one polarized along $\hat{z}$ tuned to $0_u^+(3/2)$, one polarized along $\hat{y}$ tuned to $0_g^-(3/2)$, and one polarized along $\hat{y}$ tuned to $0_g^+(1/2)$. The strengths λ_j can be tuned by adjusting the Rabi frequencies and detunings of the three fields. Using an external magnetic field and six microwave fields with, for example, frequencies and polarizations corresponding to the last six spin patterns in Table 1, arbitrary permutation-symmetric two-qubit interactions are possible.

The effective spin–spin interaction along a different intermolecular axis $\hat{z}'$ can be obtained by a frame transformation in the spherical basis. Writing $\hat{z}' = D^{1\dagger}(\beta_1, \beta_2, \beta_3)(0, 1, 0)^{\rm T}$, where D^j is the spin-j Wigner rotation, the effective hamiltonian along $\hat{z}'$ in the original coordinate system is obtained by the following replacements to the field polarization vector and spin operators: $(\alpha_-, \alpha_0, \alpha_+)^{\rm T} \to D^{1\dagger}(\beta_1, \beta_2, \beta_3)(\alpha_-, \alpha_0, \alpha_+)^{\rm T}$ and $\sigma^\alpha \to D^{1/2}(\beta_1, \beta_2, \beta_3)\sigma^\alpha D^{1/2\dagger}(\beta_1, \beta_2, \beta_3)$. For example, using a $\hat{z}$-polarized field tuned near $0_u^+(3/2)$ and a field polarized in the $\hat{x} - \hat{y}$ plane tuned near $1_u(3/2)$ creates a Heisenberg interaction between any two molecules separated by $\mathbf{r}$ with arbitrary orientation in space.

APPLICATIONS

We now show how to engineer the spin model I. Consider a system of trapped molecules in a square lattice with site coordinates in the $\hat{z} - \hat{x}$ plane $\{\bar{\mathbf{x}}_{i,j}\} = \{ib\hat{z} + jb\hat{x};\ i, j \in [1, \ell] \bigcap \mathbb{Z}\}$. Illuminate the system with a microwave field with linear polarization $\mathbf{e}_F = \cos\zeta\hat{y} + \sin\zeta\hat{x}$ and field frequency ω_F tuned such that the peak of the relative coordinate wavefunction at $r = b$ is near-resonant with the 2_g potential but far detuned from other excited states. Then the dominant interaction between nearest-neighbour molecules is of Ising type along each axis and we realize $H^{(I)}_{\rm spin}$ with $J = (\hbar|\Omega|)^2\langle 1/8(\hbar\omega_F - 2B - \gamma/2 - d^2/r^3)\rangle_{\rm rel}$. For realistic parameters, this coupling can range from 10 to 100 kHz, with the strength constrained by the trap spacing ($J \ll \hbar\omega_{\rm osc}$). The relative strength of the interactions along $\hat{z}$ and $\hat{x}$ can be changed by rotating the angle ζ of polarization out-of-plane. Interactions between more-distant neighbours are relatively weak because the far-off resonant coupling at larger r cannot distinguish the spin dependence of excited states.

Duoçot *et al.*[8] show that the ideal spin model I (for $\zeta \neq \pm\pi/2$) has a twofold degenerate ground subspace, which is gapped with weak size dependence for $\cos\zeta = 1$. The two ground states, which

Table 1 Some spin patterns that result from equation (3). The field polarization is given with respect to the intermolecular axis $\hat{z}$ and the frequency ω_F is chosen to be near-resonant with the indicated excited-state potential at the internuclear separation Δz. The sign of the interaction will depend on whether the frequency is tuned above or below resonance.

Polarization	Resonance	Spin pattern
$\hat{x}$	2_g	$\sigma^z\sigma^z$
$\hat{z}$	0_u^+	$\vec{\sigma}\cdot\vec{\sigma}$
$\hat{z}$	0_g^-	$\sigma^x\sigma^x+\sigma^y\sigma^y-\sigma^z\sigma^z$
$\hat{y}$	0_g^-	$\sigma^x\sigma^x-\sigma^y\sigma^y+\sigma^z\sigma^z$
$\hat{y}$	0_g^+	$-\sigma^x\sigma^x+\sigma^y\sigma^y+\sigma^z\sigma^z$
$(\hat{y}-\hat{x})/\sqrt{2}$	0_g^+	$-\sigma^x\sigma^y-\sigma^y\sigma^x+\sigma^z\sigma^z$
$\cos\xi\hat{x}+\sin\xi\hat{z}$	1_g	$\lambda_1(\sigma^x\sigma^z+\sigma^z\sigma^x)+\lambda_2\sigma^z\sigma^z$ $+\lambda_3(\sigma^x\sigma^x+\sigma^y\sigma^y)$
$\cos\xi\hat{y}+\sin\xi\hat{z}$	1_g	$\lambda_1(\sigma^y\sigma^z+\sigma^z\sigma^y)+\lambda_2\sigma^z\sigma^z$ $+\lambda_3(\sigma^x\sigma^x+\sigma^y\sigma^y)$

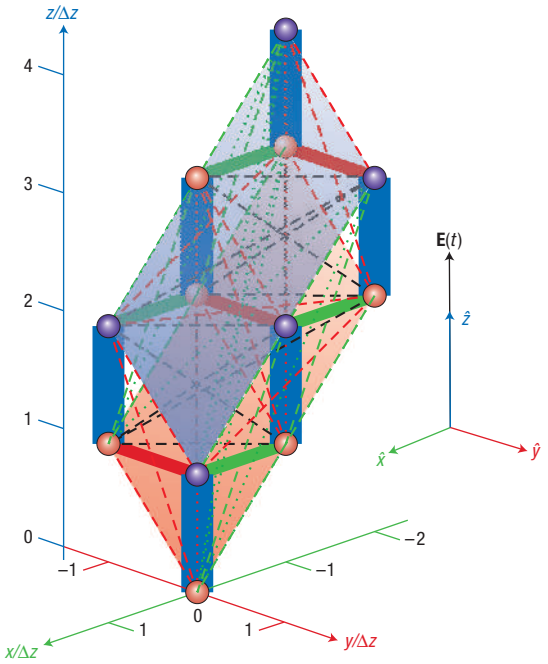

Figure 4 Implementation of spin model $H_{spin}^{(II)}$. The spatial configuration of 12 polar molecules trapped by two parallel triangular lattices (indicated by shaded planes) with separation normal to the plane of $\Delta z/\sqrt{3}$ and in-plane shift $\Delta z\sqrt{2/3}$. Nearest neighbours are separated by $\Delta z = r_\gamma$ and next-nearest-neighbour couplings are at $\sqrt{2}\Delta z$. The graph vertices represent spins and the edges correspond to pairwise spin couplings. The edge colour indicates the nature of the dominant pairwise coupling for that edge (blue $=\sigma^z\sigma^z$, red $=\sigma^y\sigma^y$, green $=\sigma^x\sigma^x$, black = 'other'). For nearest-neighbour couplings, the edge width indicates the relative strength of the absolute value of the coupling.

we denote $|0\rangle_L$ and $|1\rangle_L$, have zero local magnetizations $\langle\sigma_{i,j}^\alpha\rangle_L$. Our implementation is not ideal because there are residual longer-range interactions along several directions in the plane, as well as off-resonant couplings to excited state potentials yielding unwanted spin patterns. We note, however, that all of the effective spin hamiltonians described in equation (3) obtained using fields with linear polarization involve sums of products of Pauli operators, and are therefore invariant under time-reversal. For ℓ odd, the degeneracy present in the ground state of $H_{spin}^{(I)}$ is of Kramers' type and an imperfect implementation will not break this degeneracy, although it may decrease the energy gap.

We have numerically computed the effective interaction on a $\ell^2 = 3\times 3$ square lattice with spacings $b = r_\gamma/\sqrt{2}$, and we take the localization to the point dipole limit. In Fig. 3a we plot the $\alpha = x, y, z$-components of the r.m.s. magnetization for the ground subspace,

$$\delta^2 S^\alpha \equiv \sum_{ij}\sum_{G'G} |{}_L\langle G'|\sigma_{i,j}^\alpha|G\rangle_L|^2/2\ell^2,$$

as a function of the detuning $\omega_F - 2B/\hbar$ for polarization angle $\zeta = 0$. This allows for computation of logical qubit errors due to quasi-static noise. Near the bare resonance $\hbar\omega_F - 2B = \gamma/2$, the system shows multiple long-range resonances as all the sites couple near-resonantly at coupling strength $\propto 1/b^3$. The last of these long-range resonance appears at $\hbar\omega_F - 2B \approx 1.36\gamma$ for the interaction between next-nearest-neighbour sites with spacings of $\sqrt{2}b$. The 2_g-resonance lies at $\hbar\omega_F - 2B \approx 1.9\gamma$ for nearest-neighbour sites, and shows the remarkable feature of no magnetization on any site in any space-direction α within the ground-state manifold (see inset). The resulting immunity of the system to local noise can be probed by applying a homogeneous B-field of frequency ω_{probe} polarized in the direction $\alpha = x, y, z$. The corresponding absorption spectrum for an arbitrary code state $|\psi\rangle_L$ is

$$\chi^\alpha(\omega_{probe}) \equiv -\hbar\Gamma\Im[{}_L\langle\psi|S^\alpha(\hbar\omega_{probe} - H_{spin} + i\hbar\Gamma)^{-1}S^\alpha|\psi\rangle_L]$$

where $S^\alpha = \sum_{ij}\sigma_{i,j}^\alpha/\ell^2$ and Γ is an effective linewidth. This quantity is plotted in Fig. 3b for two different spin textures obtained for the same field frequency $\hbar\omega_F - 2B = 1.88\gamma$ but different polarizations, and where we set $\hbar\Gamma = 0.1J$. For polarization $\zeta = 0$ (see top inset) the protected qubit is realized, whose spectrum is gapped by $J/2$. For polarization along the $\hat{x}$-direction $\zeta = \pi/2$ (see bottom inset) the ground subspace is given by a set of ℓ quantum-Ising stripes along z, whose spectrum is ungapped with a large peak at $\omega_{probe} = 0$ in response to coupling with a B field polarized along $\alpha = x$.

Spin model II is similarly obtained using this mechanism. Consider a system of four molecules connected by three length-b edges forming an orthogonal triad in space. A bipartite lattice composed of such triads with equally spaced nearest neighbours can be built using two planes of stacked triangular lattices. Such a lattice could be designed using bichromatic trapping lasers in two spatial dimensions, and a suitably modulated lattice in the third dimension normal to both planes. A realization of model II using a set of three microwave fields all polarized along $\hat{z}$ is shown in Fig. 4. The interaction obtained is close to ideal with small residual coupling to next-nearest neighbours as in model I. The field detunings at the nearest-neighbour spacing are: $\hbar\omega_1 - E(1_g(1/2)) = -0.05\gamma/2$, $\hbar\omega_2 - E(0_g^-(1/2)) = 0.05\gamma/2$, $\hbar\omega_3 - E(2_g(3/2)) = 0.10\gamma/2$ and the amplitudes are $|\Omega_1| = 4|\Omega_2| = |\Omega_3| = 0.01\gamma/\hbar$. For $\gamma/h = 40$ MHz this generates effective coupling strengths $J_z/h = -100$ kHz and $J_\perp = -0.4J_z$. The magnitude of residual nearest-neighbour couplings are less than $0.04|J_z|$ along x- and y-links and less than $0.003|J_z|$ along z-links. The size of longer-range couplings J_{lr} are indicated by edge line style (dashed: $|J_{lr}| < 0.01|J_z|$, dotted: $|J_{lr}| < 10^{-3}|J_z|$). Treating pairs of spins on z-links as a single effective spin in the low-energy sector, the model approximates to Kitaev's 4-local hamiltonian[10] on

a square grid (shown here are one plaquette on the square lattice and a neighbour plaquette on the dual lattice) with an effective coupling strength $J_{\rm eff} = -(J_\perp/J_z)^4|J_z|/16 \approx h167$ Hz.

METHODS

DERIVATION OF THE MOLECULAR POTENTIALS

In the subspace of one rotational quantum ($N_1+N_2=1$), there are 24 eigenstates of $H_{\rm in}$ that are linear superpositions of two electron spin states and properly symmetrized rotational states of the two molecules. There are several symmetries that reduce $H_{\rm in}$ to block diagonal form. First, $H_{\rm dd}$, conserves the quantum number $Y = M_N + M_S$, where $M_N = M_{N_1} + M_{N_2}$ and $M_S = M_{S_1} + M_{S_2}$ are the total rotational and spin projections along the intermolecular axis. Second, parity, defined as the interchange of the two molecular cores followed by parity through the centre of each molecule, is conserved. The $\sigma = \pm 1$ eigenvalues of parity are conventionally denoted g(u) for gerade (ungerade). Finally, there is a symmetry associated with reflection R of all electronic and rotational coordinates through a plane containing the intermolecular axis. For $|Y| > 0$ all eigenstates are even under R but for states with zero angular momentum projection there are ± 1 eigenstates of R. The 16 distinct eigenvalues correspond to degenerate subspaces labelled $|Y|^{\pm}_{\sigma}(J)$ with J indicating the quantum number in the $r \to \infty$ asymptotic manifold ($N=0, J=1/2; N=1, J$).

For $Y=0$, the energies are

$$E(0^+_\sigma(1\pm 1/2)) = 2B + \gamma\left[\sigma 3x/2 - 1/4 \pm \sqrt{(\sigma x/2+1/4)^2+1/2}\right],$$

$$E(0^-_\sigma(1\pm 1/2)) = 2B + \gamma\left[-\sigma x/2 - 1/4 \pm \sqrt{(-\sigma 3x/2+1/4)^2+1/2}\right],$$

where $x \equiv d^2/\gamma r^3$. The eigenvector components are

$$K_1(0^m_\sigma) = \cos(\gamma_{O^m_\sigma}/2), \quad K_2(0^m_\sigma) = \sin(\gamma_{O^m_\sigma}/2),$$

where the angles satisfy $\tan(\gamma_{O^+_\sigma}) = \sqrt{2}/(1/2+\sigma x)$, and $\tan(\gamma_{O^-_\sigma}) = \sqrt{2}/(1/2-\sigma 3x)$. For $Y=\pm 1$ the eigenvectors and doubly degenerate eigenvalues are obtained by diagonalizing the 3×3 matrices:

$$2B\mathbf{1}_3 + \frac{\gamma}{2}\begin{pmatrix} -2\sigma x & \pm 1 & \mp 1 \\ \pm 1 & -4\sigma x & 1 \\ \mp 1 & 1 & 2\sigma x \end{pmatrix}.$$

For $Y=\pm 2$, the eigenvalues are doubly degenerate with energies $E(2_\sigma(3/2)) = 2B + \gamma/2 + \sigma\gamma x$.

THE EFFECTIVE SPIN INTERACTION

The effective spin–spin interaction, equation (3), between polar molecules depends both on the frequency $\omega_{\rm F}$ and polarization $\mathbf{e}_{\rm F} = \alpha_-\hat{e}_{-1} + \alpha_0\hat{e}_0 + \alpha_+\hat{e}_1$, ($\hat{e}_0 \equiv \hat{z}$) of the field. The explicit form for the coupling coefficients is:

$$\begin{aligned}
A_{1,1} &= |\alpha_0|^2[C(0^-_{\rm g},1,2) - C(0^+_{\rm u},1,2)] \\
&\quad + (|\alpha_-|^2 + |\alpha_+|^2)[C(1_{\rm g},3,3) - C(1_{\rm u},1,1)] \\
&\quad + \Re[\alpha^*_+\alpha_-][C(0^-_{\rm g},2,1) - C(0^+_{\rm g},2,1)], \\
A_{2,2} &= A_{1,1} - 2\Re[\alpha^*_+\alpha_-][C(0^-_{\rm g},2,1) - C(0^+_{\rm g},2,1)], \\
A_{3,3} &= |\alpha_0|^2[2C(1_{\rm g},2,2) - C(0^-_{\rm g},1,2) - C(0^+_{\rm u},1,2)] \\
&\quad + (|\alpha_+|^2 + |\alpha_-|^2)[C(2_{\rm g}) + C(0^+_{\rm g},2,1)/2 \\
&\quad + C(0^-_{\rm g},2,1)/2 - C(1_{\rm u},1,1) - C(1_{\rm g},3,3)], \\
A_{1,2} &= \Im[\alpha^*_+\alpha_-](C(0^-_{\rm g},2,1) - C(0^+_{\rm g},2,1)), \\
A_{1,3} &= \Re[\alpha^*_+\alpha_0 - \alpha^*_0\alpha_-]C(1_{\rm g},2,3), \\
A_{2,3} &= \Im[\alpha^*_+\alpha_0 - \alpha^*_0\alpha_-]C(1_{\rm g},2,3), \\
A_{0,1} &= \Re[\alpha^*_+\alpha_0 + \alpha^*_0\alpha_-]C(1_{\rm g},2,3), \\
A_{0,2} &= \Im[\alpha^*_+\alpha_0 + \alpha^*_0\alpha_-]C(1_{\rm g},2,3), \\
A_{0,3} &= (|\alpha_+|^2 - |\alpha_-|^2)[C(2_{\rm g}) - C(0^+_{\rm g},2,1)/2 - C(0^-_{\rm g},2,1)/2].
\end{aligned}$$

The component $A_{0,0}$ weights a scalar energy shift, which we ignore. The coefficients $C(|Y|^{\pm}_{\sigma})$ quantify coupling to excited states with different symmetries,

$$\begin{aligned}
C(0^m_\sigma,j,k) &= K_j(0^m_\sigma)^2 s(0^m_\sigma(3/2)) + K_k(0^m_\sigma)^2 s(0^m_\sigma(1/2)), \\
C(1_\sigma,j,k) &= \sum_{a=1}^{4} K^a_j({}^a1_\sigma(3/2))K^a_k({}^a1_\sigma(3/2))s({}^a1_\sigma(3/2)) \\
&\quad + \sum_{b=1}^{2} K^b_j({}^b1_\sigma(1/2))K^b_k({}^b1_\sigma(1/2))s({}^b1_\sigma(1/2)) \\
C(2_{\rm g}) &= s(2_{\rm g}(3/2)).
\end{aligned}$$

Here the energy-dependent terms $s(|Y|^{\pm}_{\sigma}(J)) = \hbar|\Omega|/[\hbar\omega_{\rm F} - E(|Y|^{\pm}_{\sigma}(J))]$ quantify the amplitude in the excited states. The energies $E(|Y|^{\pm}_{\sigma}(J))$ correspond to eigenvalues of $H_{\rm int}$ given above, and the sets $\{K_j(0^m_\sigma(J))\}^2_{j=1}$ and $\{K^a_j({}^a1_\sigma(J))\}^3_{j=1}$ are coefficients of the eigenvectors for $|Y|=0,1$.

A caveat is that we do not have point dipoles but rather wavepackets with spatial distributions parallel and perpendicular to the intermolecular axis $\hat{z}$. Components of intermolecular separations orthogonal to $\hat{z}$ will couple to states with different symmetry and an exact treatment would require averaging over the angular distribution with the appropriate frame transformation. However, we argue that in our regime this finite-size effect is negligible. The relative magnitude can be estimated by the ratio of the marginal relative coordinate probability distributions perpendicular and parallel to $\hat{z}$. Defining $p_\perp(r) = \int {\rm d}\Omega \sin^2\theta r^2|\psi_{\rm rel}(r,\theta)|^2$ and $p_\parallel(r) = \int {\rm d}\Omega \cos^2\theta r^2|\psi_{\rm rel}(r,\theta)|^2$, the peak of the distributions is at $r = \Delta z$, where for $z_0/\Delta z \ll 1$, the relative amount of unwanted couplings is $p_\perp(\Delta z)/p_\parallel(\Delta z) \sim 4(z_0/\Delta z)^2$. For molecular wavepacket localization $2\pi z_0/\lambda_{\rm trap} = 0.1$, the ratio is $p_\perp(\lambda_{\rm trap})/p_\parallel(\lambda_{\rm trap}) \approx 10^{-3}$, and hence it is warranted to compute the couplings as if the entire weight of the wavefunction were parallel to $\hat{z}$.

SPIN COUPLINGS AT LARGER INTERMOLECULAR RADII

Using confinement with optical lattices it may not be feasible to trap polar molecules near $\Delta z = r_\gamma$. At larger intermolecular separations where $\langle H_{\rm dd}\rangle \ll \gamma$ there is less mixing between states in different spin-rotational manifolds. However, there can still be sufficient splitting between states with different symmetries to obtain designer spin models, albeit with smaller coupling coefficents J. Consider a system with $\gamma/h = 40$ MHz and a lattice spacing $\Delta z = 5.23 r_\gamma = 300$ nm. Spin model I is built by tuning to the $2_{\rm g}$ potential with the energy $\langle 2_{\rm g}|H_{\rm int}|2_{\rm g}\rangle = 2B + \gamma/2 + d^2/r^3$. It is possible to resolve the $2_{\rm g}$ potential because the nearby $0^-_{\rm u}$ state is dark. Residual coupling between next-nearest neighbours is small as the field at $r = \sqrt{2}\Delta z$ is detuned from all resonances by at least 200 kHz. Spin model II is obtainable using a set of two microwave fields polarized along $\hat{z}$, one tuned near resonance with a $1_{\rm g}$ potential and one near a $1_{\rm u}$ potential. When the detunings and Rabi frequencies are chosen so that $\langle|\Omega_{1_{\rm g}}|C(1_{\rm g},3,3) - |\Omega_{1_{\rm u}}|C(1_{\rm u},1,1)\rangle_{\rm rel} = 0$ then the resultant spin pattern is $H^{\rm (II)}_{\rm spin}$ with $J_\perp = -\hbar\langle|\Omega_{1_{\rm g}}|C(1_{\rm g},3,3)\rangle_{\rm rel}/4$ and $J_z = \hbar\langle|\Omega_{1_{\rm g}}|C(1_{\rm g},2,2)\rangle_{\rm rel}/4$. The ratio $|J_\perp|/|J_z|$ can be tuned either by changing the lattice spacing or by using a third microwave field polarized along $\hat{z}$ and tuned near the $2_{\rm g}$ potential, in which case $J_\perp \to J_\perp + \hbar\langle|\Omega_{2_{\rm g}}|C(2_{\rm g})\rangle_{\rm rel}/8$. It is advantageous to tune fields near the 1_σ states that asymptote to the ($N=0, J=1/2; N=1, J=1/2$) manifold:

$$\begin{aligned}
\langle 1_\sigma|H_{\rm int}|1_\sigma\rangle &= 2B - \gamma - \sigma 2d^2/3r^3 \\
\langle 0^+_\sigma|H_{\rm int}|0^+_\sigma\rangle &= 2B - \gamma + \sigma 4d^2/3r^3 \\
\langle 0^-_\sigma|H_{\rm int}|0^+_\sigma\rangle &= 2B - \gamma.
\end{aligned}$$

The two field strengths $|\Omega_{1_{\rm g}}|$ and $|\Omega_{1_{\rm u}}|$ can be chosen to be nearly equal (to within less than 1%). Shifts on next-nearest neighbours are small as the field detuning at $r = \sqrt{2}\Delta z$ is at least 100 kHz.

We can define a quality factor $Q = J/h\Gamma$ quantifying the ratio of coherent coupling to the decoherence rate for the implementations above. A reasonable estimate of J for spin model I is in the range $J/h = 0.75$–7.5 kHz. This range ensures that off-resonant couplings, which give rise to interactions of different spin character are $|J_{\rm off-res}/J| = 0.01$–$0.1$. Next-nearest-neighbour interactions are $|J_{\rm nnn}/J| = 0.03$–0.3. For a decoherence rate $\Gamma \approx 0.2$ Hz, the quality factor for spin model I is then $Q = 3{,}750$–$37{,}500$. For spin model II, we find $J_\perp/h = -J_z/h = 0.16$–$1.6$ kHz, providing $|J_{\rm off-res}/J_\perp| = 0.01$–$0.1$ and

$|J_{nnn}/J_{\perp}| = 0.03$–$0.3$. This gives a quality factor $Q = 833$–$8{,}330$. These estimates were obtained without optimization.

Received 6 January 2006; accepted 27 March 2006; published 30 April 2006.

References

1. Levin, M. A. & Wen, X. G. String-net condensation: A physical mechanism for topological phases. *Phys. Rev. B* **71,** 045110 (2005).
2. Hermele, M., Fisher, M. P. A. & Balents, L. Pyrochlore photons: The $U(1)$ spin liquid in a $S = 1/2$ three-dimensional frustrated magnet. *Phys. Rev. B* **69,** 064404 (2004).
3. Einarsson, T. Fractional statistics on a torus. *Phys. Rev. Lett.* **64,** 1995–1998 (1990).
4. Jaksch, D. & Zoller, P. The cold atom Hubbard toolbox. *Ann. Phys.* **315,** 52–79 (2005).
5. Büchler, H. P., Hermele, M., Huber, S. D., Fisher, M. P. A. & Zoller, P. Atomic quantum simulator for lattice gauge theories and ring exchange models. *Phys. Rev. Lett.* **95,** 040402 (2005).
6. Santos, L. *et al.* Atomic quantum gases in kagomé lattices. *Phys. Rev. Lett.* **93,** 030601 (2004).
7. Special Issue on Ultracold Polar Molecules: Formation and Collisions. *Eur. Phys. J. D* **31,** 149–444 (2004).
8. Duoçot, B., Feigel'man, M. V., Ioffe, L. B. & Ioselevich, A. S. Protected qubits and Chern-Simons theories in Josephson junction arrays. *Phys. Rev. B* **71,** 024505 (2005).
9. Kitaev, A. Anyons in an exactly solved model and beyond. *Ann. Phys.* **321,** 2–111 (2006).
10. Dennis, E., Kitaev, A., Landahl, A. & Preskill, J. Topological quantum memory. *J. Math. Phys.* **43,** 4452–4505 (2002).
11. Duan, L. M., Demler, E. & Lukin, M. D. Controlling spin exchange interactions of ultracold atoms in optical lattices. *Phys. Rev. Lett.* **91,** 090402 (2003).
12. Sage, J. M., Sainis, S., Bergeman, T. & DeMille, D. Optical production of ultracold polar molecules. *Phys. Rev. Lett.* **94,** 203001 (2005).
13. Jaksch, D., Venturi, V., Cirac, J. I., Williams, C. J. & Zoller, P. Creation of a molecular condensate by dynamically melting a Mott insulator. *Phys. Rev. Lett.* **89,** 040402 (2002).
14. Brennen, G. K., Deutsch, I. H. & Williams, C. J. Quantum logic for trapped atoms via molecular hyperfine interactions. *Phys. Rev. A* **65,** 022313 (2002).
15. Friedrich, B. & Herschbach, D. Alignment and trapping of molecules in intense laser fields. *Phys. Rev. Lett.* **74,** 4623–4626 (1995).
16. DeMille, D. Quantum computation with trapped polar molecules. *Phys. Rev. Lett.* **88,** 067901 (2002).
17. Kotochigova, S., Tiesinga, E. & Julienne, P. S. Photoassociative formation of ultracold polar KRb molecules. *Eur. Phys. J. D* **31,** 189–194 (2004).
18. Movre, M. & Pichler, G. Resonant interaction and self-broadening of alkali resonance lines I. Adiabatic potential curves. *J. Phys. B* **10,** 2631–2638 (1977).

Acknowledgements

A.M. thanks W. Ernst, and P.Z. thanks T. Calarco, L. Faoro, M. Lukin, and D. Petrov for helpful discussions. This work was supported by the Austrian Science Foundation, the European Union, OLAQUI, SCALA and the Institute for Quantum Information.
Correspondence and requests for materials should be addressed to A.M.

Competing financial interests

The authors declare that they have no competing financial interests.